

pubs.acs.org/JPCL Letter

Ultrafast Fluctuations in PM6 Domains of Binary and Ternary Organic Photovoltaic Thin Films Probed with Two-Dimensional White-Light Spectroscopy

Zachary T. Armstrong, Miriam Bohlmann Kunz, and Martin T. Zanni*



Cite This: J. Phys. Chem. Lett. 2021, 12, 8972–8979



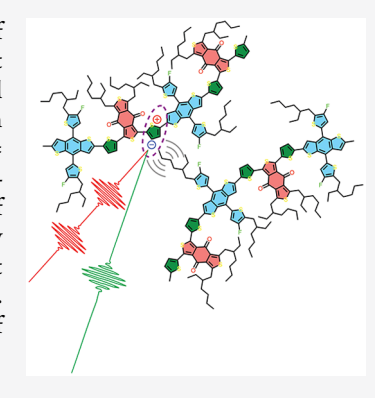
ACCESS

III Metrics & More

Article Recommendations

Supporting Information

ABSTRACT: We present two-dimensional white-light spectroscopy (2DWL) measurements of binary and ternary bulk heterojunctions of the polymer donor PM6 mixed with state-of-the-art nonfullerene acceptors Y6 or IT4F. The ternary film has a shorter lifetime and faster spectral diffusion than either of the binary films. 2D line shape analysis of the PM6 ground state bleach with a Kubo model determines that all three films have similar amplitudes of fluctuations (Δ = 0.29 fs⁻¹) in their transition frequencies, but different relaxation times (ranging from 102 to 24 fs). The ternary film exhibits faster dynamics than either of the binary films. The short lifetime of the ternary blend is consistent with increased photoexcitation transfer and the fast frequency fluctuations are consistent with structural dynamics of aliphatic side chains. These results suggest that the femtosecond fluctuations of PM6 are impacted by the choice of the acceptor molecules. We hypothesize that those dynamics are either indicative, or perhaps the initial source, of structural dynamics that ultimately contribute to solar cell operation.



Solar energy has recently seen an explosion in its application, owing to a lowering of production and installation costs of silicon solar cells, but new technologies, such as organic photovoltaics, offer the potential for easier production and more widespread use.^{2,3} Organic photovoltaics are an intriguing technology because they are solution processable and do not require high temperatures to manufacture, which simplifies production and promises a lower CO₂ footprint than silicon solar cells. Though peak efficiencies still lag behind silicon and other inorganic materials like GaAs and CdTe, single junction efficiencies of organic solar cells have recently surpassed 17.5%, largely attributed to the development of new nonfullerene acceptors such as ITIC, Y6, and their derivatives. 5-7 Continued fundamental research into the mechanisms of operation of organic solar cells will help drive new material discovery and increase device performance.

Absorption of light by the donor semiconductor leads to the formation of excitons or Coulombically bound electron hole pairs. These excitons are dissociated into free carriers via electron transfer into a second, electron accepting material, usually mixed in with the donor material in a bulk heterojunction architecture. Traditionally this acceptor material was C_{60} , PCBM, or another fullerene derivative. More recently, nonfullerene acceptors such as ITIC and Y6 (see structures in Figure 1a) lead to higher efficiencies because of better energy level alignment with the donor material (Figure 1b). In addition, ITIC and Y6 create free carriers because they absorb in the red and NIR parts of the solar spectrum (Figure 1c). $^{5-7}$ Engineering of the crystal packing of

nonfullerene acceptors has increased the charge transport efficiency in three dimensions, resulting high collection efficiencies at the electrodes.^{9,10}

The highest efficiency organic solar cells utilize a ternary design, where one donor polymer is combined with two nonfullerene acceptors. 11,12 Many ternary combinations of donor polymers and nonfullerene acceptors are possible and have been studied. 13-16 Usually, but not always, ternary films are improved over their binary counterparts, which is consistent with better coverage of the solar spectrum by including the second acceptor material. 17-21 But, a wider range of absorption cannot entirely explain the improvements in efficiency, because films with nearly identical absorption spectra have different efficiencies, suggesting that nanoscale or molecular differences also play a role. We examine the binary and ternary systems of the donor polymer PM6 (also called PBDB-T-2F) and the nonfullerene acceptors Y6 and IT4F. PM6:Y6 solar cells have been reported as high as 15.7% efficient. 13,22 Another high performing nonfullerene acceptor is IT4F, which has been used with PM6 to produce cells with efficiencies of 12.9%. 18 Li et al. fabricated ternary solar cells

Received: July 12, 2021



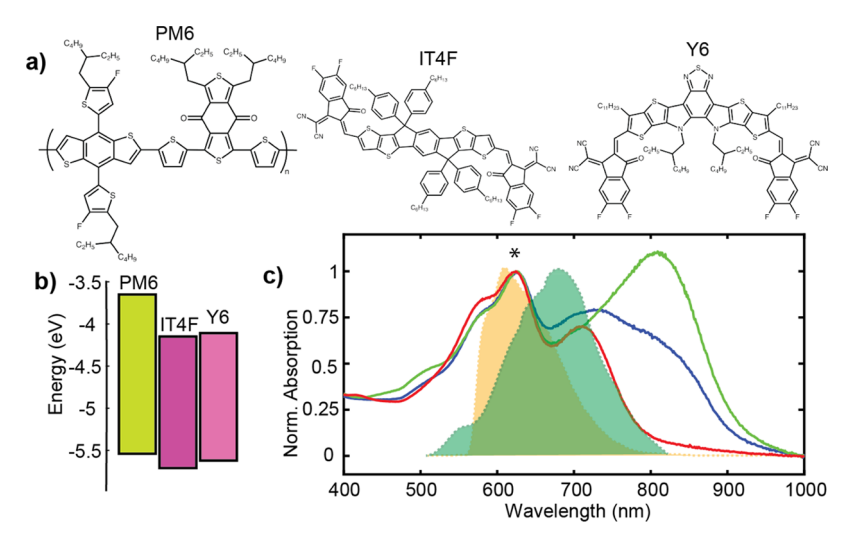


Figure 1. Compounds considered in this work. (a) Structures of compounds considered in this work. (b) Energy levels of PM6, IT4F, and Y6 taken from Li et al. ¹⁸ (c) Linear absorption spectra of PM6:IT4F (red), PM6:Y6 (green), and the ternary blend (blue) normalized to the height of the PM6 peak with the spectra of the pump (shaded orange) and probe (shaded green) pulses used for 2DES measurements.

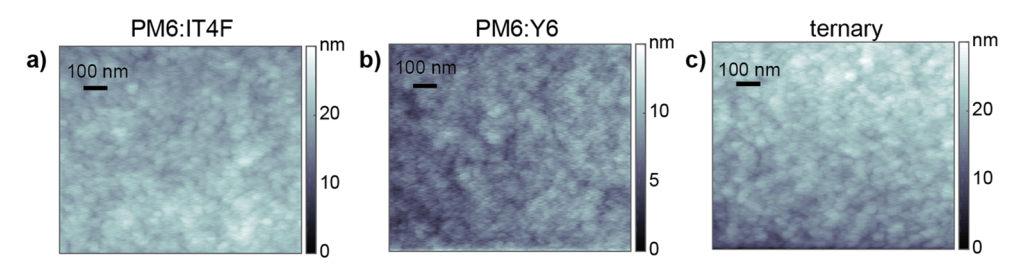


Figure 2. AFM images collected in tapping mode of PM6:IT4F, PM6:Y6, and PM6:IT4F:Y6 bulk-heterojunctions.

from these materials and found the efficiency increased to 16.5%. 18

One possible explanation for the anomalously high efficiency of the ternary film is the packing of the polymers in the domains. Bulk-heterojunctions made from a polymer donor and a nonfullerene acceptor are thought to contain crystalline domains of the donor and acceptors and an amorphous mixture of the donor and acceptor together. 23-25 The relative amount of each of these phases and their purities can influence the overall photovoltaic performance because the charge separation and transport properties of the bulk-heterojunction are extremely sensitive to the packing of the donor and acceptor materials.²⁶ Grazing incidence wide-angle X-ray scattering and resonant soft X-ray scattering measurements have shown that the packing of polymer chains within the donor domains is sensitive to the side chain size, ^{27,28} acceptor material, 18,19 and ratio of the acceptor material used in film fabrication. 23,25

Ultrafast charge transfer and other femtosecond energy transfer processes are the first processes to occur upon absorption of a photon and often play important roles in device efficiency. The time scale of these processes often correlate with materials or processing methods and differences in efficiency, open circuit voltage, current density, and other devices metrics. Several transient absorption (TA) studies of the PM6:Y6 and PM6:IT4F systems have identified hole transfer from excitons in the acceptor material to be a process that contributes to the overall photocurrent as well as electron transfer from the donor material. 19,24,25,34–37 Chen et al. varied the morphology of their bulk heterojunction films and found

that the grain size controls the hole transfer time scale.²⁵ Yang et al. found that use of solvent additives in preparation of the bulk heterojunctions can suppress recombination losses.³⁵

A more advanced form of TA spectroscopy, ultrafast twodimensional electronic spectroscopy (2DES), probes both structures, and dynamics. By measuring 2D lineshapes as a function of delay time, the magnitude and time scales of the fluctuations of the environment around the photogenerated excitons are measured, which are created by molecular differences in structure and their motions. 2DES has recently been used to study PM6:Y6 films. It was found that thermal annealing may affect coherent phonons that are thought to play an important role in the charge transfer process.²⁴ Beyond organic materials, 2DES has been used extensively in the study of perovskite solar cell materials. 38-41 Seiler et al. used line shape analysis to identify polaron formation in CsPbI₃ nanocrystals.³⁸ Lineshape analysis has been used before to study how nuclear motions of the surroundings can influence electronic relaxation processes of semiconductors^{38,42} and photosynthetic complexes. 43,44

Here, we use two-dimensional white-light spectroscopy (2DWL), a variant of 2DES with ultrabroad spectral range (Figure 1c), to study the energy and charge transfer dynamics of excitons in binary and ternary blends of PM6, IT4F, and Y6. We conclude that the ternary film has the fastest relaxation of the ground state bleach transition and the fastest fluctuation time scale. Measurement of the ultrafast dynamics and relaxation processes in these films highlight how structural dynamics could be an important factor in photovoltaic design.

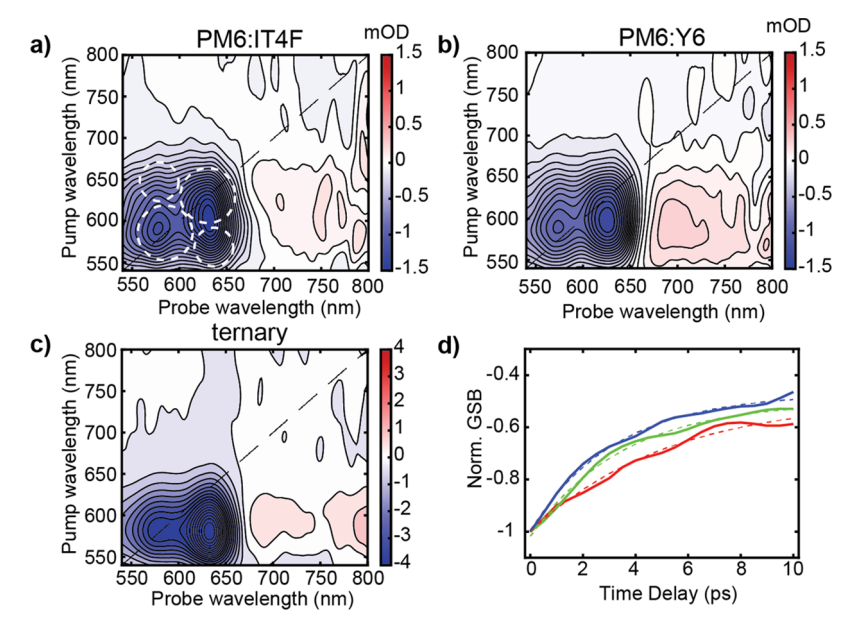


Figure 3. 2DWL spectra of PM6:IT4F (a), PM6:Y6 (b), and the ternary blend (c) at a time delay of 100 fs. Ground state bleach dynamics of the diagonal peak at 623 nm (d) for PM6:IT4F (red), PM6:Y6 (green), and the ternary blend (blue) with monoexponential fits shown as dashed lines.

Linear absorption spectra of PM6:IT4F, PM6:Y6, and the ternary blend are shown in Figure 1c. All films absorb light across the visible spectrum, with the ternary film having the broadest coverage. Thin films made solely of PM6 exhibit a strong absorption band at 623 nm with a shoulder at 580 nm which we assign to be a vibronic sideband (SI). In the mixtures, the PM6 absorption band is peaked in the same place as the PM6 control for all three films (labeled with * in Figure 1c), but in the PM6:IT4F film spectrum, the vibronic sideband is roughly 10% more intense. Electronic coupling is wellknown to modify the relative intensities of the vibronic peaks in π -stacked organic chromophores, and changes in the packing of polymer chains modulates the strength of the electronic coupling. 45,46 Thus, a different ratio is most likely indicative of different electronic couplings between the polymer chains in at least one of these films.

We used atomic force microscopy (AFM) to characterize the morphology of our bulk-heterojunctions and compared them to prior published work by others. All three films are homogeneous with grain sizes on the order of 10–20 nm (Figure 2). Our film morphologies are comparable to those of Zhu et al., I Jiang et al., and Song et al., who prepared bulk-heterojunctions with PM6 via spin-casting, as do our linear absorption spectra (Figure 1c).

2DWL spectroscopy is a third-order spectroscopy that can be thought of as a transient absorption experiment with a frequency resolved pump axis. 48,49 This extra spectral dimension allows for easier peak assignments, 50,51 monitoring of charge and energy transfer dynamics, 52,53 and analysis of spectral line shapes. 38 We use white-light supercontinua generated in YAG crystals to give us hundreds of nanometers of bandwidth for both our pump and probe pulses (Figure 1c). 54,55 Shown in Figure 3 are the 2DWL spectra of the bulk-heterojunctions considered here collected at a waiting time (pump—probe) delay of 100 fs. At 100 fs, the three spectra are qualitatively similar, with a set of negative peaks (blue) created by the ground state bleach (GSB) of PM6. There are four transitions contributing to these features: PM6 has transitions at 623 and 580 nm from the main absorption band and

vibronic sideband, respectively, which each create diagonal peaks in the 2DWL spectra. Since they share a common ground state, there are also upper and lower cross peaks between these states. We schematically draw these 4 features with white dashed circles in the PM6:IT4F spectrum (Figure 3a). We would expect to observe peaks in the NIR from the acceptor molecules at ~750 nm for IT4F or ~860 nm for Y6, but our pulses are too weak in this spectral range.

All three spectra also contain a broad positive feature (red) from excited state absorption (ESA) of PM6 excitons. This feature grows in on a 100-200 fs time scale and is present in the TA spectrum of a neat film of PM6 (SI). We note that our 2DWL spectra differ from a previously reported 2D spectrum of a PM6:Y6 film. The spectrum reported by Zhu et al. 24 contains a broad peak centered at $\sim\!620$ nm. Zhu et al. only observed a narrow excited state absorption feature after thermally annealing their films but utilized 3 nJ pulses in their experiment, which are almost 12 times stronger than our pulses. This difference in pump energy could be one explanation for differences in our measured 2D spectra. 24

In all three films, the PM6 ground state bleach peaks initially recover on a 2–4 ps time scale (Figure 3d) with additional relaxation over several hundred picoseconds. Monoexponential fits to the ground state bleach dynamics are summarized below in Table 1. To ~90% confidence, the initial decay in amplitude is fastest in the ternary film and slowest in the PM6:IT4F film.

Examining the line shape dynamics of PM6 excitons on much shorter time scales (<150 fs) reveals noticeable differences between the three films considered here. The

Table 1. Summary of Monoexponential Fitting to Ground State Bleach Relaxation^a

| film | $t_{ m GSB}~(m ps)$ |
|----------|----------------------|
| PM6:IT4F | 5.2 ± 1.3 |
| PM6:Y6 | 3.5 ± 0.5 |
| ternary | 3.2 ± 0.3 |
| | |

^aUncertainties are derived from the fits.

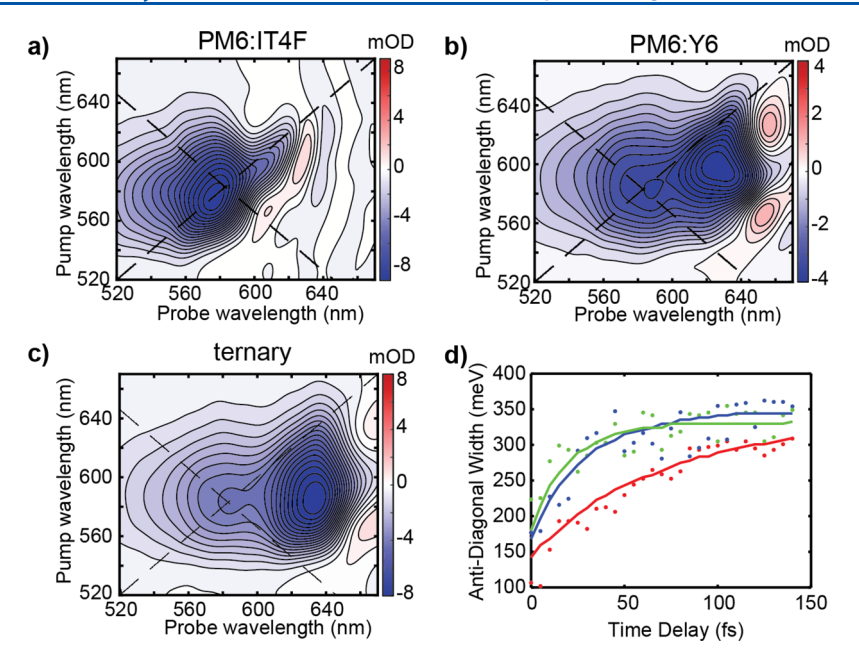


Figure 4. 2DWL spectra of PM6:IT4F (a), PM6:Y6 (b), and the ternary blend (c) at a time delay of 0 ± 5 fs. Evolution of the antidiagonal width over t_2 (d) for PM6:IT4F (red), PM6:Y6 (blue), and the ternary blend (green). Data are shown as dots with simulations from a Kubo line shape model shown as lines.

Table 2. Summary of Kubo Lineshape Simulations and Monoexponential Fitting of Antidiagonal Width Data (Figure 4d)^a

| film | $\Delta (fs^{-1})$ | au (fs) | $\Delta \Delta 	au$ | a (meV) | $t_{ m fit}$ (fs) | c (meV) | | |
|----------|--------------------|-------------|---------------------|--------------|-------------------|--------------|--|--|
| PM6:IT4F | 0.29 ± 0.01 | 102 ± 2 | 29 | 214 ± 22 | 55 ± 17 | 323 ± 24 | | |
| PM6:Y6 | 0.30 ± 0.01 | 38 ± 1 | 11 | 171 ± 38 | 30 ± 14 | 340 ± 20 | | |
| ternary | 0.29 ± 0.01 | 24 ± 1 | 7 | 106 ± 29 | 33 ± 22 | 337 ± 18 | | |
| | | | | | | | | |

^aUncertainties are derived from the fits.

elongation of the 2D line shape resolves the homogeneous from the inhomogeneous line width. If the line widths broaden as a function of the waiting time (t_2) , then spectral diffusion occurs upon excitation, revealing the time scales for exciton diffusion as well as the electronic and structural dynamics of the film. ^{38,56,57} We analyzed the antidiagonal width along the entire wavelength range. We found that the antidiagonal width at 580 nm has the least interference from the excited state absorption. By fitting the ground state bleach and excited state absorption peaks and comparing the experimental width to the width of the fitted ground state bleach peak, we estimate that the excited state absorption alters the antidiagonal widths <2% at this wavelength. Center line slope (CLS) analysis was less reliable because of the overlapping transitions. ^{38,57}

The evolution of the antidiagonal widths over t_2 is shown in Figure 4d, along with simulations of the data using the Kubo ansatz for the frequency fluctuation correlation function (FFCF):

$$\langle \delta \omega(t) \delta \omega(0) \rangle = \Delta^2 e^{-|t|/\tau} \tag{1}$$

where Δ is the magnitude and τ is the time scale of the fluctuations. For each time delay, we simulated a 2D spectrum using the FFCF from eq 1 to calculate the response functions and Fourier transformed along both dimensions to mimic the experimental measurements, from which the antidiagonal line shape is extracted. More details about the simulations are given in the SI. Δ and τ were varied until the simulated antidiagonal line widths match the experiment. The line shape dynamics were also fit with monoexponentials for a comparison of time

scales irrespective of the fits. Results of the line shape analysis and monoexponential fitting are shown in Table 2. The fluctuation amplitudes (Δ) of each of these films are almost identical at ~0.30 fs⁻¹ (1242 meV) whereas the time scales of these fluctuations (τ) are quite different for each of the films, varying by a factor of 4. Moreover, τ is inversely proportional to the photovoltaic efficiencies reported in ref 14. All three films are in the inhomogeneous limit ($\Delta\Delta\tau$ > 1), which is reflected in the elongation of the diagonal peaks in the 2DWL spectra in Figure 4.

Taken together, the 2D spectra quantify the photophysics of these films via their electronic-state lifetimes and the magnitude and dynamics of the frequency fluctuations. Regarding the lifetimes, all the ground state bleach dynamics shown in Figure 3d and summarized in Table 1 are faster than the ground state bleach dynamics of a pure film of PM6, as measured by transient absorption (SI). This increased rate in ground state bleach decay means there is a new relaxation process present in the mixed films that decreases the population of PM6 excitons created by the pump pulse. A recent study has proposed this process could either be electron transfer, which would decrease the stimulated emission pathway; or energy transfer followed by hole transfer from the acceptor,⁵⁸ which would deplete the ground state bleach pathway. In principle, we can distinguish between these two pathways with their intensities, but in practice, we cannot tell the difference because we do not observe the appearance of any new features within our spectral range. Thus, we refer to the process that depletes the intensity of the diagonal peak as "charge transfer", keeping in mind that it could also be energy

transfer. Charge transfer is known to be highly efficient ^{13,18,22} in these photovoltaic films and has been previously measured to be ultrafast. ^{24,25,34,35} Thus, one likely reason for faster dynamics is electron transfer from PM6 excitons to the acceptor molecules.

The line shape dynamics are caused by a thermal bath of the vibrations of the polymer. We describe this bath with the Kubo form of the frequency fluctuation correlation function (eq 1). Regarding the magnitude and time scale of the frequency fluctuations, the line width of the electronic transitions are created by structural packing of the films, structural and electronic relaxation upon photoexcitation, and other effects that change the electronic structure of the molecule. The fact that Δ is the same for all three films is consistent with the simple fact that the donor polymer, PM6, in which the exciton is created upon photoexcitation, is the same in all three films. Resonant soft X-ray scattering measurements of PM6:Y6 films by Zhu et al. showed a high degree of domain purity, meaning that we expect that a majority of the signal that we measure are from domains of relatively pure (~96%) PM6.²⁴ Therefore, the excitons created in PM6 are exposed to the same environment and structural distribution, regardless of the mixture.

The other observation of interest is that the time scales (τ) for the frequency fluctuations scale inversely with the expected efficiency of the devices that are made from films of this type. The sub-100-fs time scale for all of the films measured here is consistent with the inertial component often seen in ultrafast measurements that measure dynamics and reflect the strength of the system-environment coupling. 59-63 For example, it has been commonly observed that dye molecules exhibit different line shape dynamics in solvents of different polarity. 64,65 Because of the similarity in time scales, we attribute the spectral diffusion observed here to similar forces. Indeed, the structures of other semiconducting polymers fluctuate on similar time scales. Guilbert et al. simulated the molecular dynamics of P3HT aggregates and calculated correlation functions for several different structural parameters. They found that motion of the backbone has a correlation time of several nanoseconds, the beginning and middle part of the alkyl side chains have correlation times of several picoseconds, and the ends of the side chains have femtosecond correlation times. 66 We would expect similar time scales for the alkyl side chain motion of PM6 (Figure 1a). The PM6 excitons are likely concentrated in the aromatic backbone, but the time scales suggest that the packing of the PM6 backbones brings them into contact with the side chains. The fact that these time scales differ for each of the mixtures, suggests that the structural dynamics of PM6 is influenced by the choice of acceptors.

Other explanations for the line shape dynamics shown in Figure 4 could be diffusion (exciton hopping) or delocalization. If the excitons hop faster than the environment around them can fluctuate, the inhomogeneously broadened peaks will become rounder during t_2 , similar to what we observe in Figure 4. However, Jiang et. al measured the diffusion length in PM6 films to be ~7 nm. ⁶⁷ Assuming a monomer length of 21 Å, the hopping time to a neighboring site is 26 ps which is much slower than the <100 fs line shape dynamics we observe. Delocalization of the excitons is presumably also impacted by the dephasing rate. Because disorder causes localization, exciton delocalization, static structural disorder, and structural dynamics are interconnected. ^{68,69}

We have studied the dynamics of excitons in PM6 incorporated into binary and ternary bulk-heterojunctions with the nonfullerene acceptors IT4F and Y6 using twodimensional white-light (2DWL) spectroscopy. We have found that the ternary blend exhibits the fastest relaxation of the ground state bleach peak (t_{GSB}) , which we assign to be charge transfer to the acceptors. The ternary film also has the fastest line shape dynamics (τ) , indicating that the femtosecond dynamics of PM6, which we assign to aliphatic side chain motions, are impacted by the choice of acceptor. Modeling the 2DWL lineshapes directly from molecular dynamics simulations of PM6 would help determine more precisely what ultrafast motions are present and how they influence the exciton dynamics. In the future, it should be possible to resolve cross peaks between the donor and acceptors, allowing for simultaneous monitoring of electron and hole transfer dynamics and confirmation of these charge transfer times. Lineshape analysis of donor-acceptor cross peaks could help determine to what extent the fluctuations measured here influence other ultrafast processes in these films.

ASSOCIATED CONTENT

Supporting Information

The Supporting Information is available free of charge at https://pubs.acs.org/doi/10.1021/acs.jpclett.1c02234.

Experimental methods, linear absorption spectra of solutions and neat films, transient absorption spectra of neat films, and additional details about line shape simulations (PDF)

AUTHOR INFORMATION

Corresponding Author

Martin T. Zanni — Department of Chemistry, University of Wisconsin—Madison, Madison, Wisconsin 53706, United States; orcid.org/0000-0001-7191-9768; Email: zanni@chem.wisc.edu

Authors

Zachary T. Armstrong — Department of Chemistry, University of Wisconsin—Madison, Madison, Wisconsin 53706, United States; © orcid.org/0000-0002-1207-6171

Miriam Bohlmann Kunz – Department of Chemistry, University of Wisconsin—Madison, Madison, Wisconsin 53706, United States

Complete contact information is available at: https://pubs.acs.org/10.1021/acs.jpclett.1c02234

Notes

The authors declare the following competing financial interest(s): M.T.Z. is a co-owner of PhaseTech Spectroscopy, which sells ultrafast pulse shapers and multidimensional spectrometers.

ACKNOWLEDGMENTS

We thank Sean M. Foradori and Michael S. Arnold for assistance with sample preparation. Funding was provided by the National Science Foundation (NSF CHE 1954700). M.B.K. is grateful for support from the National Science Foundation Graduate Research Fellowship Program under grant no. DGE-1747503. M.T.Z. is a co-owner of PhaseTech Spectroscopy which sells ultrafast pulse shapers and multi-dimensional spectrometers.

REFERENCES

- (1) Nemet, G. F. How Solar Energy Became Cheap: A Model for Low-Carbon Innovation; Routledge, 2019.
- (2) Leo, K. Organic Photovoltaics. *Nat. Rev. Mater.* **2016**, *1* (8), 1–2.
- (3) Lewis, N. S. Research Opportunities to Advance Solar Energy Utilization. *Science* **2016**, *351* (6271), aad1920.
- (4) Best Research-Cell Efficiency Chart. https://www.nrel.gov/pv/cell-efficiency.html (accessed 2020-11-24).
- (5) Li, S.; Li, C.-Z.; Shi, M.; Chen, H. New Phase for Organic Solar Cell Research: Emergence of Y-Series Electron Acceptors and Their Perspectives. *ACS Energy Lett.* **2020**, *5* (5), 1554–1567.
- (6) Zhang, J.; Tan, H. S.; Guo, X.; Facchetti, A.; Yan, H. Material Insights and Challenges for Non-Fullerene Organic Solar Cells Based on Small Molecular Acceptors. *Nat. Energy* **2018**, 3 (9), 720–731.
- (7) Hou, J.; Inganäs, O.; Friend, R. H.; Gao, F. Organic Solar Cells Based on Non-Fullerene Acceptors. *Nat. Mater.* **2018**, *17* (2), 119–128.
- (8) Classen, A.; Chochos, C. L.; Lüer, L.; Gregoriou, V. G.; Wortmann, J.; Osvet, A.; Forberich, K.; McCulloch, I.; Heumüller, T.; Brabec, C. J. The Role of Exciton Lifetime for Charge Generation in Organic Solar Cells at Negligible Energy-Level Offsets. *Nat. Energy* **2020**, *5* (9), 711–719.
- (9) Zhou, J.; Wen, X.; Tang, N.; Zhou, X.; Wang, C.; Zheng, N.; Liu, L.; Xie, Z. Ultrafast and Long-Range Exciton Migration through Anisotropic Coulombic Coupling in the Textured Films of Fused-Ring Electron Acceptors. *J. Phys. Chem. Lett.* **2020**, *11* (18), 7908–7913.
- (10) Firdaus, Y.; Le Corre, V. M.; Karuthedath, S.; Liu, W.; Markina, A.; Huang, W.; Chattopadhyay, S.; Nahid, M. M.; Nugraha, M. I.; Lin, Y.; Seitkhan, A.; Basu, A.; Zhang, W.; McCulloch, I.; Ade, H.; Labram, J.; Laquai, F.; Andrienko, D.; Koster, L. J. A.; Anthopoulos, T. D. Long-Range Exciton Diffusion in Molecular Non-Fullerene Acceptors. *Nat. Commun.* **2020**, *11* (1), 5220.
- (11) An, Q.; Zhang, F.; Zhang, J.; Tang, W.; Deng, Z.; Hu, B. Versatile Ternary Organic Solar Cells: A Critical Review. *Energy Environ. Sci.* **2016**, 9 (2), 281–322.
- (12) Xie, Y.; Yang, F.; Li, Y.; Uddin, M. A.; Bi, P.; Fan, B.; Cai, Y.; Hao, X.; Woo, H. Y.; Li, W.; Liu, F.; Sun, Y. Morphology Control Enables Efficient Ternary Organic Solar Cells. *Adv. Mater.* **2018**, *30* (38), 1803045.
- (13) Song, J.; Li, C.; Zhu, L.; Guo, J.; Xu, J.; Zhang, X.; Weng, K.; Zhang, K.; Min, J.; Hao, X.; Zhang, Y.; Liu, F.; Sun, Y. Ternary Organic Solar Cells with Efficiency > 16.5% Based on Two Compatible Nonfullerene Acceptors. *Adv. Mater.* **2019**, *31* (52), 1905645.
- (14) Ma, R.; Liu, T.; Luo, Z.; Gao, K.; Chen, K.; Zhang, G.; Gao, W.; Xiao, Y.; Lau, T.-K.; Fan, Q.; Chen, Y.; Ma, L.-K.; Sun, H.; Cai, G.; Yang, T.; Lu, X.; Wang, E.; Yang, C.; Jen, A. K.-Y.; Yan, H. Adding a Third Component with Reduced Miscibility and Higher LUMO Level Enables Efficient Ternary Organic Solar Cells. ACS Energy Lett. 2020, 5 (8), 2711–2720.
- (15) Gao, J.; Gao, W.; Ma, X.; Hu, Z.; Xu, C.; Wang, X.; An, Q.; Yang, C.; Zhang, X.; Zhang, F. Over 14.5% Efficiency and 71.6% Fill Factor of Ternary Organic Solar Cells with 300 Nm Thick Active Layers. *Energy Environ. Sci.* 2020, 13 (3), 958–967.
- (16) Liu, T.; Luo, Z.; Chen, Y.; Yang, T.; Xiao, Y.; Zhang, G.; Ma, R.; Lu, X.; Zhan, C.; Zhang, M.; Yang, C.; Li, Y.; Yao, J.; Yan, H. A Nonfullerene Acceptor with a 1000 Nm Absorption Edge Enables Ternary Organic Solar Cells with Improved Optical and Morphological Properties and Efficiencies over 15%. *Energy Environ. Sci.* 2019, 12 (8), 2529–2536.
- (17) Gasparini, N.; Salleo, A.; McCulloch, I.; Baran, D. The Role of the Third Component in Ternary Organic Solar Cells. *Nat. Rev. Mater.* **2019**, *4* (4), 229–242.
- (18) Li, K.; Wu, Y.; Tang, Y.; Pan, M.-A.; Ma, W.; Fu, H.; Zhan, C.; Yao, J. Ternary Blended Fullerene-Free Polymer Solar Cells with 16.5% Efficiency Enabled with a Higher-LUMO-Level Acceptor to

- Improve Film Morphology. Adv. Energy Mater. 2019, 9 (33), 1901728.
- (19) Wang, B.; Fu, Y.; Yang, Q.; Wu, J.; Li, Y.; Sharma, G. D.; Keshtov, M. L.; Xie, Z. Impacts of a Second Acceptor on the Energy Loss, Blend Morphology and Carrier Dynamics in Non-Fullerene Ternary Polymer Solar Cells. *J. Mater. Chem. C* **2020**, 8 (34), 11727—11734.
- (20) Jiang, B.-H.; Chen, C.-P.; Liang, H.-T.; Jeng, R.-J.; Chien, W.-C.; Yu, Y.-Y. The Role of Y6 as the Third Component in Fullerene-Free Ternary Organic Photovoltaics. *Dyes Pigm.* **2020**, *181*, 108613.
- (21) Zhan, L.; Li, S.; Lau, T.-K.; Cui, Y.; Lu, X.; Shi, M.; Li, C.-Z.; Li, H.; Hou, J.; Chen, H. Over 17% Efficiency Ternary Organic Solar Cells Enabled by Two Non-Fullerene Acceptors Working in an Alloylike Model. *Energy Environ. Sci.* **2020**, *13* (2), 635–645.
- (22) Yuan, J.; Zhang, Y.; Zhou, L.; Zhang, G.; Yip, H.-L.; Lau, T.-K.; Lu, X.; Zhu, C.; Peng, H.; Johnson, P. A.; Leclerc, M.; Cao, Y.; Ulanski, J.; Li, Y.; Zou, Y. Single-Junction Organic Solar Cell with over 15% Efficiency Using Fused-Ring Acceptor with Electron-Deficient Core. *Joule* 2019, 3 (4), 1140–1151.
- (23) Hamid, Z.; Wadsworth, A.; Rezasoltani, E.; Holliday, S.; Azzouzi, M.; Neophytou, M.; Guilbert, A. A. Y.; Dong, Y.; Little, M. S.; Mukherjee, S.; Herzing, A. A.; Bristow, H.; Kline, R. J.; DeLongchamp, D. M.; Bakulin, A. A.; Durrant, J. R.; Nelson, J.; McCulloch, I. Influence of Polymer Aggregation and Liquid Immiscibility on Morphology Tuning by Varying Composition in PffBT4T-2DT/Nonfullerene Organic Solar Cells. *Adv. Energy Mater.* 2020, 10 (8), 1903248.
- (24) Zhu, W.; Spencer, A. P.; Mukherjee, S.; Alzola, J. M.; Sangwan, V. K.; Amsterdam, S. H.; Swick, S. M.; Jones, L. O.; Heiber, M. C.; Herzing, A. A.; Li, G.; Stern, C. L.; DeLongchamp, D. M.; Kohlstedt, K. L.; Hersam, M. C.; Schatz, G. C.; Wasielewski, M. R.; Chen, L. X.; Facchetti, A.; Marks, T. J. Crystallography, Morphology, Electronic Structure, and Transport in Non-Fullerene/Non-Indacenodithienothiophene Polymer:Y6 Solar Cells. *J. Am. Chem. Soc.* 2020, 142 (34), 14532—14547.
- (25) Chen, Z.; Chen, X.; Qiu, B.; Zhou, G.; Jia, Z.; Tao, W.; Li, Y.; Yang, Y. M.; Zhu, H. Ultrafast Hole Transfer and Carrier Transport Controlled by Nanoscale-Phase Morphology in Nonfullerene Organic Solar Cells. J. Phys. Chem. Lett. 2020, 11 (9), 3226–3233.
- (26) Movaghar, B.; Jones, L. O.; Ratner, M. A.; Schatz, G. C.; Kohlstedt, K. L. Are Transport Models Able To Predict Charge Carrier Mobilities in Organic Semiconductors? *J. Phys. Chem. C* **2019**, 123 (49), 29499–29512.
- (27) Awartani, O. M.; Gautam, B.; Zhao, W.; Younts, R.; Hou, J.; Gundogdu, K.; Ade, H. Polymer Non-Fullerene Solar Cells of Vastly Different Efficiencies for Minor Side-Chain Modification: Impact of Charge Transfer, Carrier Lifetime, Morphology and Mobility. *J. Mater. Chem. A* **2018**, *6* (26), 12484–12492.
- (28) Wang, G.; Swick, S. M.; Matta, M.; Mukherjee, S.; Strzalka, J. W.; Logsdon, J. L.; Fabiano, S.; Huang, W.; Aldrich, T. J.; Yang, T.; Timalsina, A.; Powers-Riggs, N.; Alzola, J. M.; Young, R. M.; DeLongchamp, D. M.; Wasielewski, M. R.; Kohlstedt, K. L.; Schatz, G. C.; Melkonyan, F. S.; Facchetti, A.; Marks, T. J. Photovoltaic Blend Microstructure for High Efficiency Post-Fullerene Solar Cells. To Tilt or Not To Tilt? J. Am. Chem. Soc. 2019, 141 (34), 13410–13420.
- (29) Piris, J.; Dykstra, T. E.; Bakulin, A. A.; van Loosdrecht, P. H. M.; Knulst, W.; Trinh, M. T.; Schins, J. M.; Siebbeles, L. D. A. Photogeneration and Ultrafast Dynamics of Excitons and Charges in P3HT/PCBM Blends. *J. Phys. Chem. C* **2009**, *113* (32), 14500–14506.
- (30) Voss, M. G.; Scholes, D. T.; Challa, J. R.; Schwartz, B. J. Ultrafast Transient Absorption Spectroscopy of Doped P3HT Films: Distinguishing Free and Trapped Polarons. *Faraday Discuss.* **2019**, 216 (0), 339–362.
- (31) Grzegorczyk, W. J.; Savenije, T. J.; Dykstra, T. E.; Piris, J.; Schins, J. M.; Siebbeles, L. D. A. Temperature-Independent Charge Carrier Photogeneration in P3HT-PCBM Blends with Different Morphology. *J. Phys. Chem. C* **2010**, *114* (11), 5182–5186.

- (32) Tamai, Y.; Fan, Y.; Kim, V. O.; Ziabrev, K.; Rao, A.; Barlow, S.; Marder, S. R.; Friend, R. H.; Menke, S. M. Ultrafast Long-Range Charge Separation in Nonfullerene Organic Solar Cells. *ACS Nano* **2017**, *11* (12), 12473–12481.
- (33) Liu, J.; Chen, S.; Qian, D.; Gautam, B.; Yang, G.; Zhao, J.; Bergqvist, J.; Zhang, F.; Ma, W.; Ade, H.; Inganäs, O.; Gundogdu, K.; Gao, F.; Yan, H. Fast Charge Separation in a Non-Fullerene Organic Solar Cell with a Small Driving Force. *Nat. Energy* **2016**, *1* (7), 1–7.
- (34) Wang, R.; Zhang, C.; Li, Q.; Zhang, Z.; Wang, X.; Xiao, M. Charge Separation from an Intra-Moiety Intermediate State in the High-Performance PM6:Y6 Organic Photovoltaic Blend. *J. Am. Chem. Soc.* **2020**, *142* (29), 12751–12759.
- (35) Yang, Q.; Li, X.; Tang, H.; Li, Y.; Fu, Y.; Li, Z.; Xie, Z. Ultrafast Spectroscopic Investigation of the Effect of Solvent Additives on Charge Photogeneration and Recombination Dynamics in Non-Fullerene Organic Photovoltaic Blends. *J. Mater. Chem. C* **2020**, 8 (20), 6724–6733.
- (36) Gao, J.; Ming, R.; An, Q.; Ma, X.; Zhang, M.; Miao, J.; Wang, J.; Yang, C.; Zhang, F. Ternary Organic Solar Cells with J71 as Donor and Alloyed Acceptors Exhibiting 13.16% Efficiency. *Nano Energy* **2019**, *63*, 103888.
- (37) Tang, H.; Xu, T.; Yan, C.; Gao, J.; Yin, H.; Lv, J.; Singh, R.; Kumar, M.; Duan, T.; Kan, Z.; Lu, S.; Li, G. Donor Derivative Incorporation: An Effective Strategy toward High Performance All-Small-Molecule Ternary Organic Solar Cells. *Adv. Sci.* **2019**, *6* (21), 1901613.
- (38) Seiler, H.; Palato, S.; Sonnichsen, C.; Baker, H.; Socie, E.; Strandell, D. P.; Kambhampati, P. Two-Dimensional Electronic Spectroscopy Reveals Liquid-like Lineshape Dynamics in CsPbI 3 Perovskite Nanocrystals. *Nat. Commun.* **2019**, *10* (1), 4962.
- (39) Nguyen, X. T.; Timmer, D.; Rakita, Y.; Cahen, D.; Steinhoff, A.; Jahnke, F.; Lienau, C.; De Sio, A. Ultrafast Charge Carrier Relaxation in Inorganic Halide Perovskite Single Crystals Probed by Two-Dimensional Electronic Spectroscopy. *J. Phys. Chem. Lett.* **2019**, 10 (18), 5414–5421.
- (40) Richter, J. M.; Branchi, F.; Valduga de Almeida Camargo, F.; Zhao, B.; Friend, R. H.; Cerullo, G.; Deschler, F. Ultrafast Carrier Thermalization in Lead Iodide Perovskite Probed with Two-Dimensional Electronic Spectroscopy. *Nat. Commun.* **2017**, 8 (1), 376.
- (41) Zhao, W.; Qin, Z.; Zhang, C.; Wang, G.; Dai, X.; Xiao, M. Coherent Exciton-Phonon Coupling in Perovskite Semiconductor Nanocrystals Studied by Two-Dimensional Electronic Spectroscopy. *Appl. Phys. Lett.* **2019**, *115* (24), 243101.
- (42) Singh, R.; Moody, G.; Siemens, M. E.; Li, H.; Cundiff, S. T. Quantifying Spectral Diffusion by the Direct Measurement of the Correlation Function for Excitons in Semiconductor Quantum Wells. *J. Opt. Soc. Am. B* **2016**, 33 (7), C137–C143.
- (43) Wong, C. Y.; Alvey, R. M.; Turner, D. B.; Wilk, K. E.; Bryant, D. A.; Curmi, P. M. G.; Silbey, R. J.; Scholes, G. D. Electronic Coherence Lineshapes Reveal Hidden Excitonic Correlations in Photosynthetic Light Harvesting. *Nat. Chem.* **2012**, *4* (5), 396–404.
- (44) Rolczynski, B. S.; Yeh, S.-H.; Navotnaya, P.; Lloyd, L. T.; Ginzburg, A. R.; Zheng, H.; Allodi, M. A.; Otto, J. P.; Ashraf, K.; Gardiner, A. T.; Cogdell, R. J.; Kais, S.; Engel, G. S. Time-Domain Line-Shape Analysis from 2D Spectroscopy to Precisely Determine Hamiltonian Parameters for a Photosynthetic Complex. *J. Phys. Chem. B* **2021**, *125* (11), 2812–2820.
- (45) Hestand, N. J.; Spano, F. C. Interference between Coulombic and CT-Mediated Couplings in Molecular Aggregates: H- to J-Aggregate Transformation in Perylene-Based π -Stacks. J. Chem. Phys. **2015**, 143 (24), 244707.
- (46) Hestand, N. J.; Spano, F. C. Expanded Theory of H- and J-Molecular Aggregates: The Effects of Vibronic Coupling and Intermolecular Charge Transfer. *Chem. Rev.* **2018**, *118* (15), 7069–7163.
- (47) Duan, L.; Zhang, Y.; Yi, H.; Haque, F.; Deng, R.; Guan, H.; Zou, Y.; Uddin, A. Trade-Off between Exciton Dissociation and Carrier Recombination and Dielectric Properties in Y6-Sensitized

- Nonfullerene Ternary Organic Solar Cells. Energy Technol. 2020, 8 (1), 1900924.
- (48) Hamm, P.; Zanni, M. Concepts and Methods of 2D Infrared Spectroscopy; Cambridge University Press, 2011.
- (49) Shim, S.-H.; Zanni, M. T. How to Turn Your Pump-Probe Instrument into a Multidimensional Spectrometer: 2D IR and Vis Spectroscopiesvia Pulse Shaping. *Phys. Chem. Chem. Phys.* **2009**, *11* (5), 748-761.
- (50) Jones, A. C.; Kearns, N. M.; Ho, J.-J.; Flach, J. T.; Zanni, M. T. Impact of Non-Equilibrium Molecular Packings on Singlet Fission in Microcrystals Observed Using 2D White-Light Microscopy. *Nat. Chem.* **2020**, *12* (1), 40–47.
- (51) Armstrong, Z. T.; Kunz, M. B.; Jones, A. C.; Zanni, M. T. Thermal Annealing of Singlet Fission Microcrystals Reveals the Benefits of Charge Transfer Couplings and Slip-Stacked Packing. *J. Phys. Chem. C* **2020**, *124* (28), 15123–15131.
- (52) Flach, J. T.; Wang, J.; Arnold, M. S.; Zanni, M. T. Providing Time to Transfer: Longer Lifetimes Lead to Improved Energy Transfer in Films of Semiconducting Carbon Nanotubes. *J. Phys. Chem. Lett.* **2020**, *11* (15), 6016–6024.
- (53) Mehlenbacher, R. D.; McDonough, T. J.; Grechko, M.; Wu, M.-Y.; Arnold, M. S.; Zanni, M. T. Energy Transfer Pathways in Semiconducting Carbon Nanotubes Revealed Using Two-Dimensional White-Light Spectroscopy. *Nat. Commun.* **2015**, *6* (1), 1–7.
- (54) Kearns, N. M.; Mehlenbacher, R. D.; Jones, A. C.; Zanni, M. T. Broadband 2D Electronic Spectrometer Using White Light and Pulse Shaping: Noise and Signal Evaluation at 1 and 100 kHz. *Opt. Express* **2017**, 25 (7), 7869–7883.
- (55) Jones, A. C.; Kearns, N. M.; Bohlmann Kunz, M.; Flach, J. T.; Zanni, M. T. Multidimensional Spectroscopy on the Microscale: Development of a Multimodal Imaging System Incorporating 2D White-Light Spectroscopy, Broadband Transient Absorption, and Atomic Force Microscopy. *J. Phys. Chem. A* **2019**, *123* (50), 10824–10836
- (56) Segarra-Martí, J.; Segatta, F.; Mackenzie, T. A.; Nenov, A.; Rivalta, I.; Bearpark, M. J.; Garavelli, M. Modeling Multidimensional Spectral Lineshapes from First Principles: Application to Water-Solvated Adenine. *Faraday Discuss.* **2020**, *221* (0), 219–244.
- (57) Nemeth, A.; Milota, F.; Mančal, T.; Lukeš, V.; Kauffmann, H. F.; Sperling, J. Vibronic Modulation of Lineshapes in Two-Dimensional Electronic Spectra. *Chem. Phys. Lett.* **2008**, 459 (1), 94–99.
- (58) Karuthedath, S.; Gorenflot, J.; Firdaus, Y.; Chaturvedi, N.; De Castro, C. S. P.; Harrison, G. T.; Khan, J. I.; Markina, A.; Balawi, A. H.; Peña, T. A. D.; Liu, W.; Liang, R.-Z.; Sharma, A.; Paleti, S. H. K.; Zhang, W.; Lin, Y.; Alarousu, E.; Anjum, D. H.; Beaujuge, P. M.; De Wolf, S.; McCulloch, I.; Anthopoulos, T. D.; Baran, D.; Andrienko, D.; Laquai, F. Intrinsic Efficiency Limits in Low-Bandgap Non-Fullerene Acceptor Organic Solar Cells. *Nat. Mater.* **2021**, *20* (3), 378–384.
- (59) Rosenthal, S. J.; Xie, X.; Du, M.; Fleming, G. R. Femtosecond Solvation Dynamics in Acetonitrile: Observation of the Inertial Contribution to the Solvent Response. *J. Chem. Phys.* **1991**, 95 (6), 4715–4718.
- (60) Rosenthal, S. J.; Jimenez, R.; Fleming, G. R.; Kumar, P. V.; Maroncelli, M. Solvation Dynamics in Methanol: Experimental and Molecular Dynamics Simulation Studies. *J. Mol. Liq.* **1994**, *60* (1), 25–56.
- (61) Bolzonello, L.; Polo, A.; Volpato, A.; Meneghin, E.; Cordaro, M.; Trapani, M.; Fortino, M.; Pedone, A.; Castriciano, M. A.; Collini, E. Two-Dimensional Electronic Spectroscopy Reveals Dynamics and Mechanisms of Solvent-Driven Inertial Relaxation in Polar BODIPY Dyes. J. Phys. Chem. Lett. 2018, 9 (5), 1079–1085.
- (62) Lee, Y.; Das, S.; Malamakal, R. M.; Meloni, S.; Chenoweth, D. M.; Anna, J. M. Ultrafast Solvation Dynamics and Vibrational Coherences of Halogenated Boron-Dipyrromethene Derivatives Revealed through Two-Dimensional Electronic Spectroscopy. *J. Am. Chem. Soc.* 2017, 139 (41), 14733–14742.

- (63) Fortino, M.; Collini, E.; Pedone, A.; Bloino, J. Role of Specific Solute—Solvent Interactions on the Photophysical Properties of Distyryl Substituted BODIPY Derivatives. *Phys. Chem. Chem. Phys.* **2020**, 22 (19), 10981—10994.
- (64) Moca, R.; Meech, S. R.; Heisler, I. A. Two-Dimensional Electronic Spectroscopy of Chlorophyll a: Solvent Dependent Spectral Evolution. *J. Phys. Chem. B* **2015**, *119* (27), 8623–8630.
- (65) Burt, J. A.; Zhao, X.; McHale, J. L. Inertial Solvent Dynamics and the Analysis of Spectral Line Shapes: Temperature-Dependent Absorption Spectrum of β-Carotene in Nonpolar Solvent. *J. Chem. Phys.* **2004**, 120 (9), 4344–4354.
- (66) Guilbert, A. A. Y.; Zbiri, M.; Dunbar, A. D. F.; Nelson, J. Quantitative Analysis of the Molecular Dynamics of P3HT:PCBM Bulk Heterojunction. J. Phys. Chem. B 2017, 121 (38), 9073–9080.
- (67) Jiang, K.; Zhang, J.; Peng, Z.; Lin, F.; Wu, S.; Li, Z.; Chen, Y.; Yan, H.; Ade, H.; Zhu, Z.; Jen, A. K.-Y. Pseudo-Bilayer Architecture Enables High-Performance Organic Solar Cells with Enhanced Exciton Diffusion Length. *Nat. Commun.* **2021**, *12* (1), 468.
- (68) Barford, W.; Trembath, D. Exciton Localization in Polymers with Static Disorder. *Phys. Rev. B: Condens. Matter Mater. Phys.* **2009**, 80 (16), 165418.
- (69) Simine, L.; Rossky, P. J. Relating Chromophoric and Structural Disorder in Conjugated Polymers. *J. Phys. Chem. Lett.* **2017**, 8 (8), 1752–1756.